Progress In Electromagnetics Research C, Vol. 122, 267–277, 2022

A Slotted Compact Four-Port Truncated Ground Structured MIMO Antenna for Sub-6 3.4 GHz 5G Application

Rayirathil K. Athira Mohan and Kanagasabapathi G. Padmasine*

Abstract—A novel high performance four-port multiple input multiple output antenna is suggested for 5G application functioning at 3.4 GHz band. The antenna design measures an inclusive volume of $32\,\text{mm} \times 32\,\text{mm} \times 0.8\,\text{mm}^3$. The broad frequency bandwidth, excellent gain, decreased interelement gap, and effective isolation within the MIMO components of the proposed system are clearly novel. Each antenna in the four-element MIMO system has been situated orthogonally to the others while maintaining a small size and good result. The antenna has exceptional average total efficiency in the 5G sub-6 GHz spectrum and is in good agreement with the measured results. It also offers a high realized gain compared to prior MIMO antennas. The antenna has a high impedance matching whose isolation is about −28 dB, computed envelope correlation coefficient smaller than 0.10, channel capacity loss average value less than 0.2 bits per second per hertz, and the diversity gain about 10 dB. The typical peak realized antenna gain of the offered MIMO antenna is also delivered with a high radiation efficiency at the frequency of 3.4 GHz. The reflection coefficient, mutual coupling, radiation pattern, current distribution, and gain of antennas are all measured and explained. The design has a compact high volume and adequate bandwidth with good accomplished gain making the antenna very strong for 5G application.

1. INTRODUCTION

Multiple-input multiple-output (MIMO) communication systems use various antenna sectors during transmission and reception to improve reliability over different antenna configurations in multipath propagation. The antenna attributes, as well as the multipath channel description, are important factors influencing communication performance in such systems. While source code and signal processing are essential parts of a MIMO system's implementation, the propagation frequency and antenna design are significant factors that eventually influence system performance. As a result, a huge amount of research has gone into these two categories. Evaluating the possibilities of MIMO systems, for example, necessitates a new degree of knowledge about multipath channel characteristics [1]. Industries and academia are concentrating more on establishing MIMO antenna systems as the necessity for high data rates and increase in large channel capacity. Multiband functionality, increased bandwidth, greater gain or efficiency, strong channel capacity, and diversity effectiveness are the main objectives of the MIMO system [2]. MIMO antenna technology has been advocated as a way to accomplish high-quality data transmission and has become a popular choice among antenna designers. A successful MIMO antenna, on the other hand, should satisfy several critical criteria, including sufficient isolation between elements, better bandwidth features, and high-performance individual elements [3, 4]. As a result, MIMO technology has been actively explored and implemented in order to improve system throughput and transmission power. One of the most stimulating problems in the MIMO framework is achieving optimal inaccessibility and moderate correlation among separate aspects, which could

Received 21 May 2022, Accepted 7 August 2022, Scheduled 17 August 2022
* Corresponding author: Kanagasabapathi Girirajan Padmasine (padmasine@buc.edu.in).
The authors are with the Department of Electronics and Instrumentation, Bharathiar University, Coimbatore, Tamil Nadu, India.

enhance channel capacity and as more than just a result, achieve both a higher gain and a higher spectral efficiency [5]. The most basic approach to reduce mutual interference is to organize and structure antenna parts (typically half wavelength distance). Despite the fact that this technology solves the bonding problem, it necessitates such a broad implementation area that it is inappropriate for use in hand-held wireless access due to space limitations. As an outcome, numerous methods for reducing inter-element interaction and thus promoting isolation have been developed in recent years in order to increase overall functionality and reliability. The potential data rate efficiency in wireless network would be quadrupled and enhanced within the multiple-input multiple-output system [6]. By implementing MIMO synthesis and improving the utilization of the transmission spectrum and power, extra connections can be exploited to enhance network throughput [7]. One of the most efficient methods in the next 5G mobile communication is MIMO technology. Multiple antennas placed in ground stations and communication devices simultaneously can boost signal quality within a particular frequency spectrum. The 3500 MHz (3400–3600 MHz) range was designated as a new 5G communication channel in 2015. Since then, both commercial and academic researches have flourished in this area.

One of the trendiest topics in 5G MIMO is multiple antenna design. To ensure that the wireless channels are independent, high port isolation between elements is required [8]. To create a large number of users, upcoming mobile communication will necessitate a higher data rate and more capacity. Because the signal in a multipath environment is progressively suppressed, getting a higher Signal to Noise Ratio (SNR) is a difficult challenge. The antenna's gain could be boosted even further to improve the SNR value. The active aperture area of the antenna is directly proportional to its gain. To attain optimum gain, a single antenna with a bigger aperture area is recommended [9–11]. Even in a multipath environment, the space diversity strategy used in MIMO antennas considerably boosts the transmitted signal and gain [12]. In this situation of a MIMO antenna, the separation between the antennas should be considerable. High data rates, minimal latency, and massive bandwidth are all advantages of 5G communication [13, 14]. In 5G, there are two types of frequency bands: (i) below 6 GHz and (ii) above 20 GHz to 80 GHz in many bands. Due to the need for existing wireless communication technology, the sub-6 GHz band can be used instantly. For 5G connectivity, the sub-6 GHz frequency band ranges from 3.4 to 3.6 GHz. In this work, a compact MIMO system is proposed where four elements are used with feeding techniques operating at 3.4 GHz frequency band functioning in the frequency range 3400–3600 MHz. The 4-port MIMO system is considered and constructed on an FR4 substrate. The paper is arranged in the following pattern. The concept, design, and operating mechanisms of the innovative MIMO antenna are covered in Section 2. The equivalent circuit model, simulated and measured environments, as well as the outcomes, are covered in Section 3. At last, the current distribution is covered, and the conclusion is given.

2. CONCEPT OF THE DESIGNED ANTENNA

2.1. Single Antenna Design and Analysis

The suggested single antenna structure and design strategy are completely covered in this section. Moreover, the scattering parameters, gain, and overall efficiency of the measured and simulated results are closely examined. The antenna model is constructed on an FR4 Epoxy substrate with a low dielectric constant level and a thickness of 0.8 mm. This design is produced and modeled using Ansys HFSS electromagnetic simulation software and CST Studio package 2019.

2.2. Single Antenna Geometry and Its Design Procedures

The proposed layout and design concept for a single-element antenna are seen in this technique. The antenna consists of a radiating patch with a feed line and a copper ground plane as mentioned above, and it resonates with a reasonable bandwidth according to the well-established mathematical equation.

$$P_w = \frac{C}{2f_r}\sqrt{\frac{2}{\gamma_r + 1}} \tag{1}$$

$$P_L = \frac{C}{2f_r\sqrt{\gamma_{eff}}} - 2\Delta L \tag{2}$$

where the patch length and width are represented as P_L and P_w; C denotes the speed of light; γ_r is the dielectric constant of the given substrate; γ_{eff} indicates the effective dielectric value of the radiating patch; and ΔL denotes the change in patch length. The suggested antenna's impedance bandwidth and impedance matching are enhanced by moving the feed line's location to the right. The antenna covered the sub-6 GHz frequency range in 5G in this phase and displayed exceptional operational bandwidth of 3.4 GHz. The radiating patch's corner square plots are etched in the following step. The suggested design's front and bottom viewpoints are shown, along with the final optimized intended design characteristics.

2.3. Design of Overall Antenna Geometry

Figure 1 explains the planned antenna, which comprises four P-shaped monopole antenna elements. On an FR-4 dielectric substrate, the intended 3.4 GHz MIMO antenna is built. With a total substrate size

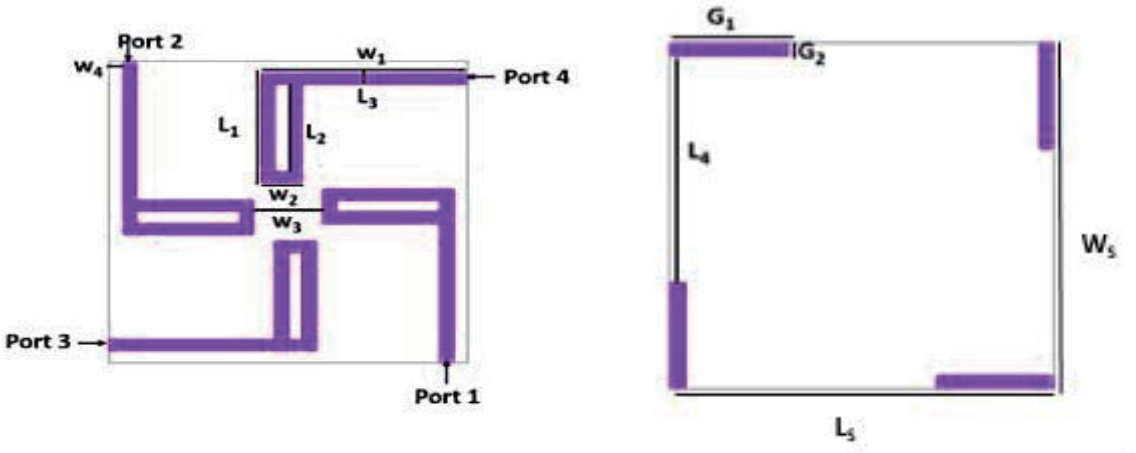

Figure 1. Designed antenna with partial ground.

Table 1. A comparing result of different 5G MIMO antennas.

Reference	Operating Frequency (GHz)	Number of Ports	Measurements (mm^3)	Isolation (dB)	ECC	Peak gain (dBi)	Efficiency (%)
[8]	2.4 GHz	2	$22 \times 12 \times 6$	−10 dB	0.015	NG	NG
[9]	3.1–3.8 and 4.8–6 GHz	8	$17.85 \times 5 \times 0.8$	−10 dB	less than 0.06	NG	65%–75% (LB) and 60%–71% (HB)
[10]	3.3–4.2, 3.3–3.8 and 4.4–5 GHz	4	$120 \times 65 \times 1.6$	−18.8 dB	Lower than 0.018	4.71 dBi	NG
[11]	2.4 GHz	4	$26 \times 26 \times 0.8$	−25 dB	0.02	2.4 dBi	77%
[12]	2.4 GHz	2	$30 \times 44 \times 1.6$	−35 dB	0.02	1.4 dBi	85%
[13]	3.6 GHz	8	$136 \times 68 \times 1$	−11.7 dB	Less than 0.1	NG	NG
[14]	2.3 and 4.2 GHz	4	$44 \times 44 \times 0.8$	−24.8 dB	NG	NG	NG
This work	**3.4 GHz**	**4**	**$32 \times 32 \times 0.8$**	**−28 dB**	**Less than 0.1**	**3.2 dBi**	**82%**

NG* = Not Given.

of $32 \times 32 \times 0.8\,\text{mm}^3$, the suggested configuration of the four division MIMO antenna is recognized as the lowest possible design in 5G antennas. As depicted in Figure 1, the microstrip design is considered as a particular 50-ohm microstrip line that is constructed and created on an FR-4 material. At first, only one of the antenna elements was considered. At the required frequency, the antenna's dimensions were optimized as 3.4 GHz. Figure 2(a) shows a simulated reflection coefficient of the single antenna element. Figure 2(b) shows the antenna's simulated and measured return losses. As seen in the figures, the simulated and measured findings had nearly the same resonance frequency as shown in Figures 2(c) and (d). The constructed prototypes bandwidth is lower than the derived prototypes, but it is still greater than the needed band. With a separation spacing, the four p-shaped portions are symmetrically positioned. The absolutely tiny ground area is engraved on the lower side of the material when this nomenclature is used. Each radiating element's ground plane was split into four rectangular sections made below it. The conceptual outlooks of the assessed radiating element which is in the front part and partial ground which is on the back side, as well as the optimum size, are shown in Figure 1. With the help of Ansys HFSS, the current design is simulated. Table 1 shows the comparison of different 5G MIMO antennas, and Table 2 lists the geometrical parameters in detail, along with their values.

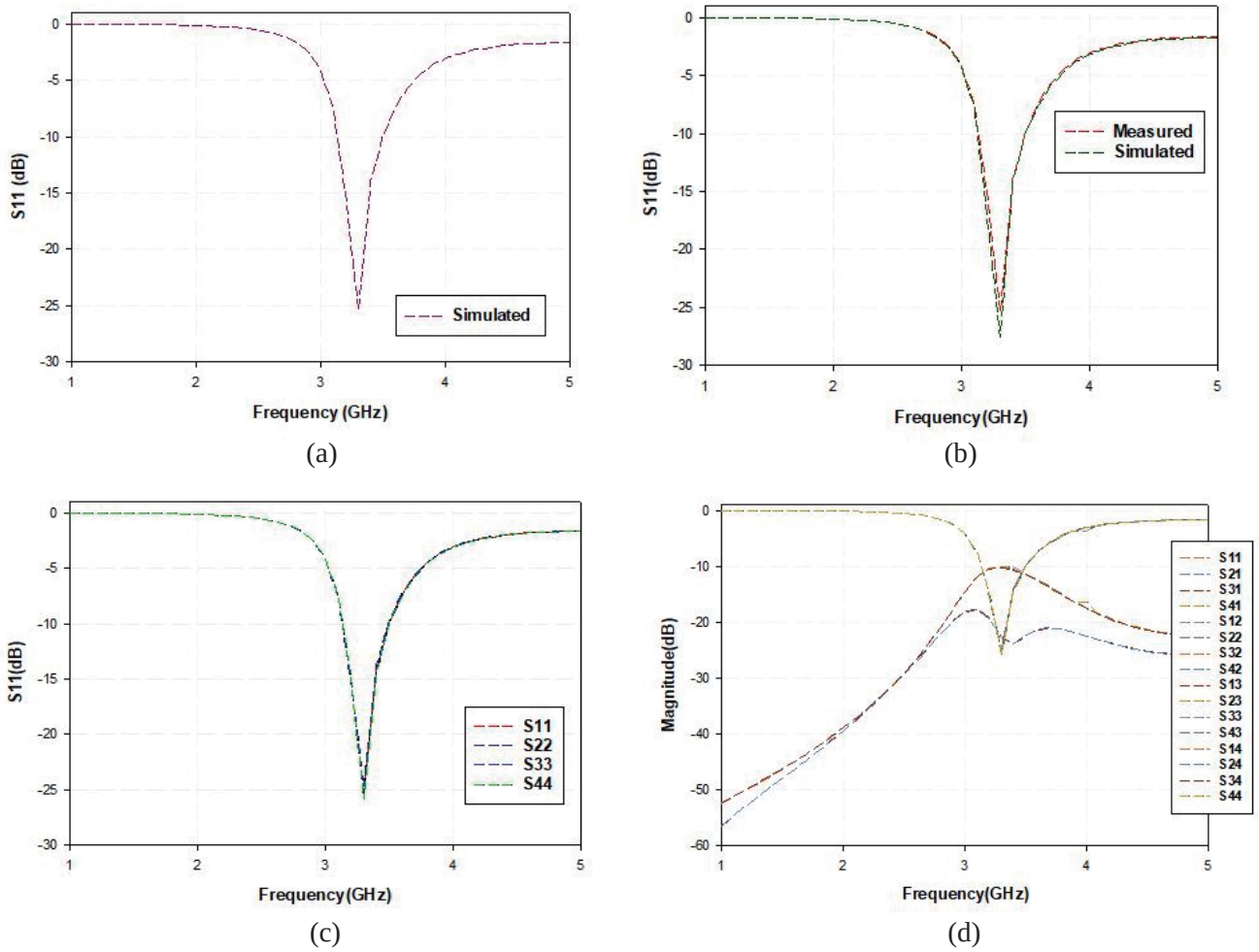

Figure 2. (a) Simulated Reflection coefficient of a single antenna. (b) Simulated and Measured S-parameter. (c) Simulated results of a proposed MIMO antenna with all ports. (d) Isolation Performance of the suggested antenna.

Table 2. Optimized design parameters of the designed antenna.

Parameter	Description	Value
W_1	Width of the feedline	15 mm
W_2	Width of the patch	2 mm
L_1	Length of the patch	13 mm
L_2	Length of the slot	11 mm
L_3	Length of the feedline	1 mm
G_1	Length of the ground	8 mm
G_2	Width of the ground	1 mm
L_S	Length of the substrate	32 mm
W_S	Width of the substrate	32 mm

2.4. Simulated and Measured Results of the Antenna

On an FR4 substrate, the desired four-port MIMO antenna system was set up. The foremost and backmost surfaces of the manufactured MIMO antenna prototype are presented. Input impedance, mutual coupling between antenna elements, efficiency, radiation characteristics, and envelop correlation coefficient are all performance measures included in the following statement.

Figure 2 depicts the designed simulated and measured S-parameters. At 3.4 GHz, the projected design has a modelled normal frequency range, with isolations around -28 dB between adjoining and diagonal ports. This approach is demonstrated using the antenna configuration depicted in Figure 2. This antenna was produced on a 0.8 mm thick FR-4 substrate. Four rectangular copper elements were fabricated beneath each radiating element to simulate the antenna's ground area. There are totally four connectors used to feed the four port radiators, as indicated in the given figure. With just a slight shift in the resonant frequency, the observed S-parameters of the proposed configuration are in satisfactory correlation with the simulated findings, which can be attributed by a range of factors including manufacturing method and error, along with port/cable connection losses. Because the least interaction between specific radiating elements is necessarily tied to the antenna diversity efficiency, the isolation seen between elements of the recommended antenna was researched and evaluated. In the above figure, it shows the simulated and experimental isolation results of the antenna. In the projected antenna's impedance band, the isolation values fluctuate. The results suggest that MIMO applications around 3.4 GHz can work well, with isolation stronger than -20 dB.

2.5. Electric Current Distribution

The outcomes of the mutual connection between the radiating features of the antenna design are validated using the figures above. This can be related to the surface current distribution of the antenna as shown in Figure 3. For instance, one of the four ports should be activated to investigate the effect of connectivity between antenna segments using this technique, while the other three ports should indeed be stopped with a 50-ohm load, as shown in Figure 3. When calculating how often the antennas are apart, the distance between the ports is essential. When the antenna elements are divided by a large distance, there is a substantial level of isolation. Only port 1 is active, as shown in Figure 3(a). On the feeding part, the current concentrations have become more intense as illustrated in Figure 3(a), as there is no current associated with the adjoining ports.

As a result, S_{12} (or S_{34}) isolation parameter can be used to assess its influence. Only this port has current when the second port is activated, and the other ports are disconnected with a 50 load. When port 3 and port 4 are stimulated, a similar condition is portrayed in Figures 3(c) and 3(d). As seen in the figures, the surface current is generally intensive over the stimulated port. As a result, the observed and simulated isolations of the suggested antenna in figures are significant at 10 dB. The E- and H-planes at 3.4 GHz are employed to explore the antenna emission patterns when one port is activated, and the others are fitted to a 50-ohm load, as illustrated in Figure 4.

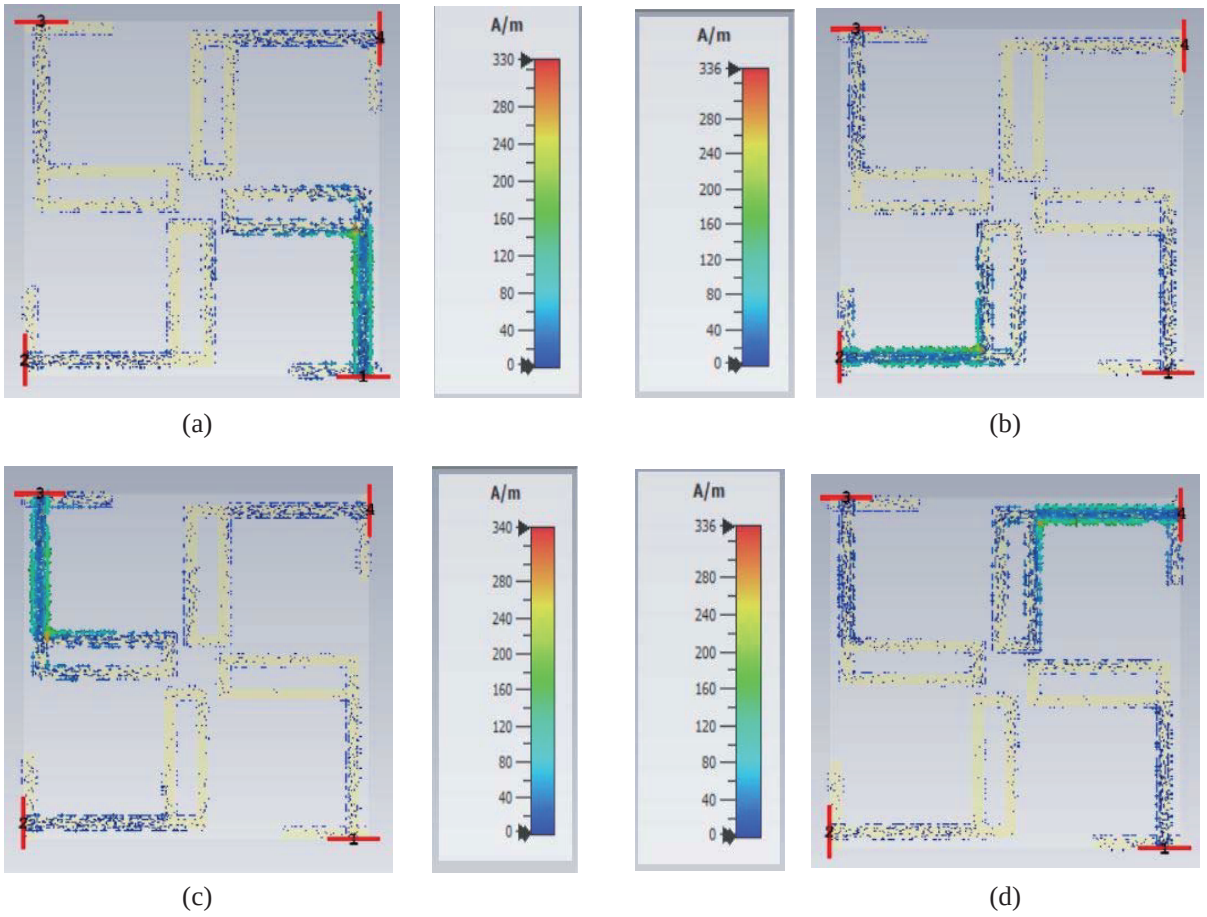

Figure 3. Surface current distribution at 3.4 GHz, excitation of (a) port 1, (b) port 2, (c) port 3, (d) port 4.

Both the planes are generated field patterns of the current MIMO antenna which are displayed at the 3.4 GHz resonant frequencies provided by the Ansys HFSS software, as indicated. The computed radiation is acquired and accomplished inside an anechoic chamber to measure the received field when a conventional horn antenna is used as a transmitter and a power meter. One port is specified to perform as a receiver throughout the measurement technique, while the subsequent ports are saturated with a 50-ohm load to inhibit signal pickup. This step is repeated for each of the MIMO design ports that have been offered. The antenna performance is expressed in relation to the reflection coefficients, gain, and radiation pattern. The suggested antenna gain is a far-field characteristic that is tested using two standard antennas and the suggested architecture in an anechoic chamber. Figure 5 shows the measured and simulated gain at 3.4 GHz.

Equations (1) and (2) show reflection (S_{11}/S_{22}) and transmission coefficients (S_{12}/S_{21}) using source impedance (Z_S) and load impedance (Z_L).

$$\text{Reflection Coefficient} = \frac{Z_L - Z_S}{Z_L + Z_S} \tag{3}$$

$$\text{Transmission Coefficient} = \frac{2Z_L}{Z_L + Z_S} \tag{4}$$

As shown in Equation (3), the radiation pattern can be shown as a graphical representation of generated power as a function of a coordinate space. The far-field radiation intensity is:

$$U = r^2 W_{rad} = B_o F(\theta, \phi) \cong \frac{r^2}{\eta} \left[|E_\theta(r, \theta, \phi)|^2 + |E_\theta(r, \theta, \phi)|^2 \right] \tag{5}$$

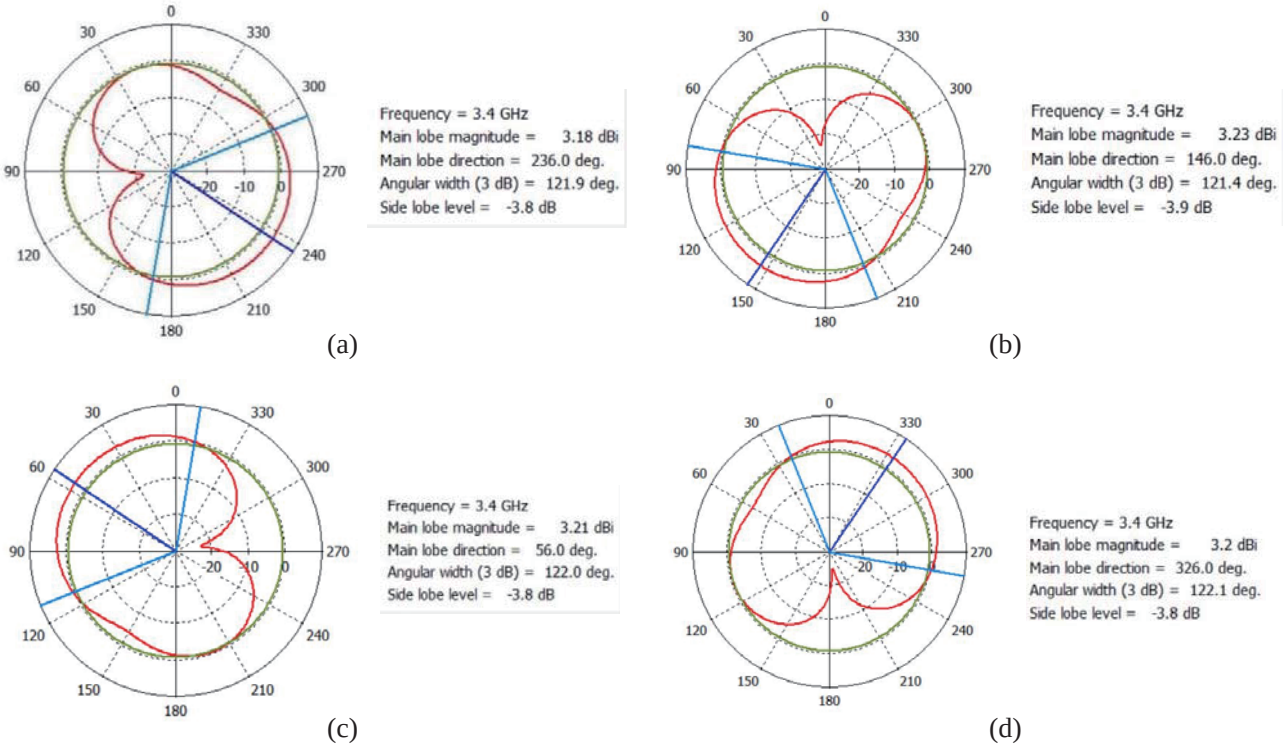

Figure 4. Radiation pattern of the projected antenna.

where,

U is the intensity of the radiation which is expressed in W/unit solid angle.

W_{rad} is the radiation density having the unit W/m^2.

$E(r, \theta, \phi)$ is the antenna's electric field intensity in the far zone.

E_θ and E_ϕ are the far zone electric field components of antenna.

η is the intrinsic impedance of the medium.

The radiation pattern of the proposed MIMO structure for the frequency 3.4 GHz is shown in Figure 4. The image depicts highly bidirectional and omnidirectional patterns for ϕ polarized elements (0 and 90 degrees) in the two major planes E and H.

The determined Envelope Correlation Coefficient (ECC) seen between ports of the designed work in all the circumstances is shown in Figure 6. In perspective of radiation pattern, this depicts how independent the various components of the antenna system are. Each element in this antenna system should always be separate from the others; yet, in reality, achieving a zero value is challenging. The three ECC readings in this case may be obtained by replacing the necessary terms into the following formula, as shown in calculations of Eqs. (6)–(8):

$$\rho_{e12} = \frac{\left|S_{11}S_{12} + S_{12}S_{22} + S_{13}S_{32} + S_{14}S_{42}\right|^2}{\left(1 - \left(\left|S_{11}\right|^2 + \left|S_{12}\right|^2\right) + \left(\left|S_{13}\right|^2 + \left|S_{14}\right|^2\right)\right)^2} \tag{6}$$

$$\rho_{e13} = \frac{\left|S_{11}S_{13} + S_{12}S_{23} + S_{13}S_{33} + S_{14}S_{43}\right|^2}{\left(1 - \left(\left|S_{11}\right|^2 + \left|S_{12}\right|^2\right) + \left(\left|S_{13}\right|^2 + \left|S_{14}\right|^2\right)\right)^2} \tag{7}$$

$$\rho_{e14} = \frac{\left|S_{11}S_{14} + S_{12}S_{24} + S_{13}S_{34} + S_{14}S_{44}\right|^2}{\left(1 - \left(\left|S_{11}\right|^2 + \left|S_{12}\right|^2\right) + \left(\left|S_{13}\right|^2 + \left|S_{14}\right|^2\right)\right)^2} \tag{8}$$

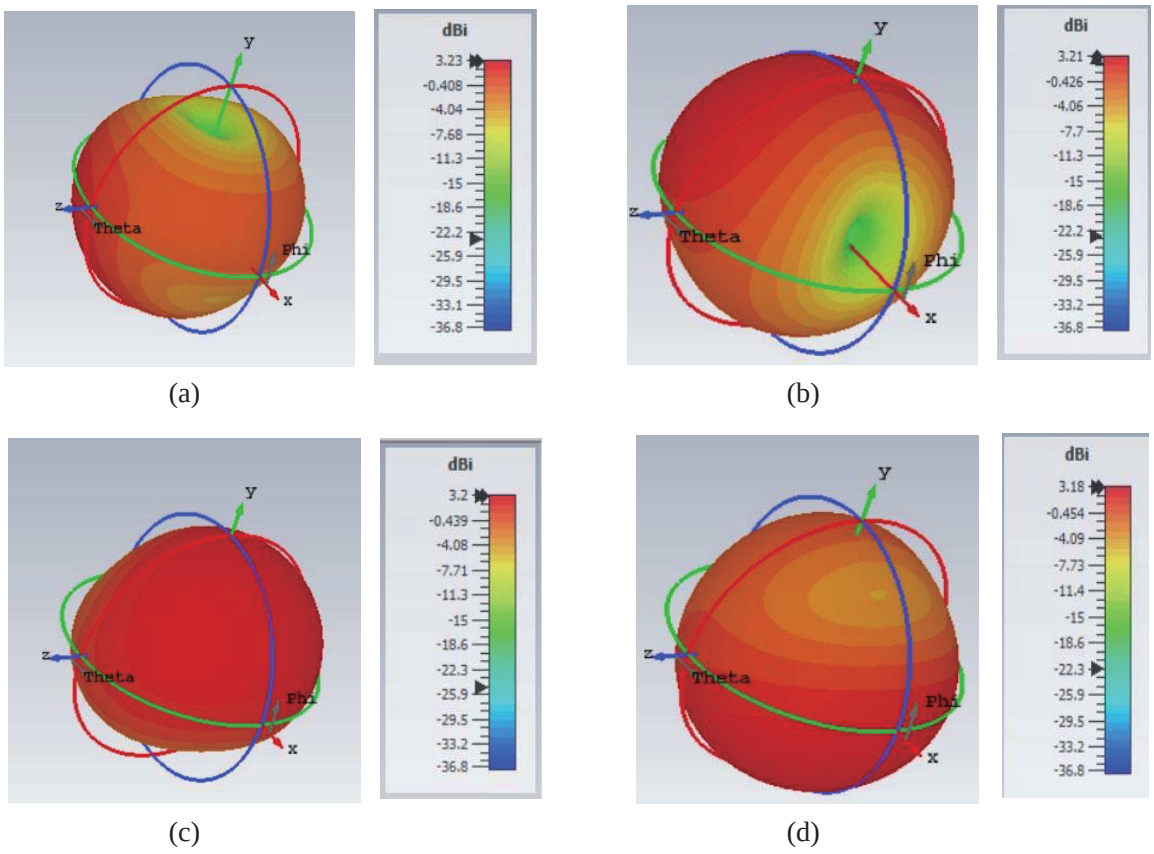

Figure 5. 3D polar plot of the proposed antenna.

The Diversity Gain (DG) is also considered as a significant diversity characteristic, which may be calculated using Equations (9)–(11) on account of increased possible DG and correlation coefficient. Any diversity method that optimizes the signal-to-interference ratio is described as diversity gain. The antenna gives excellent isolation because it has a higher distribution gain value, and vice versa. The equations express the representations of the diversity gain of the current antenna and also show that the DG values for both scenarios are around 10 dB at the functional band.

$$DG_{12} = 10\sqrt{1 - |\rho e12|^2} \tag{9}$$

$$DG_{13} = 10\sqrt{1 - |\rho e13|^2} \tag{10}$$

$$DG_{14} = 10\sqrt{1 - |\rho e14|^2} \tag{11}$$

The channel capacity loss is the maximum amount of data that may be carried without loss through a communication channel. A system design channel capacity can be presumably improved by increasing the number of antennas. The occurrence of Rayleigh-fading channels, meanwhile, will lead to a decrease in channel capacity. The channel capacity loss in a 2×2 MIMO system can be obtained from the following equation, assuming that only the receiving antenna layouts are correlated and the worst-case scenario of a high signal-to-noise ratio.

$$CCL = -\log_2 \det\left(\varphi^R\right)$$

where φ^R is referred to as the receiving antenna correlation matrix.

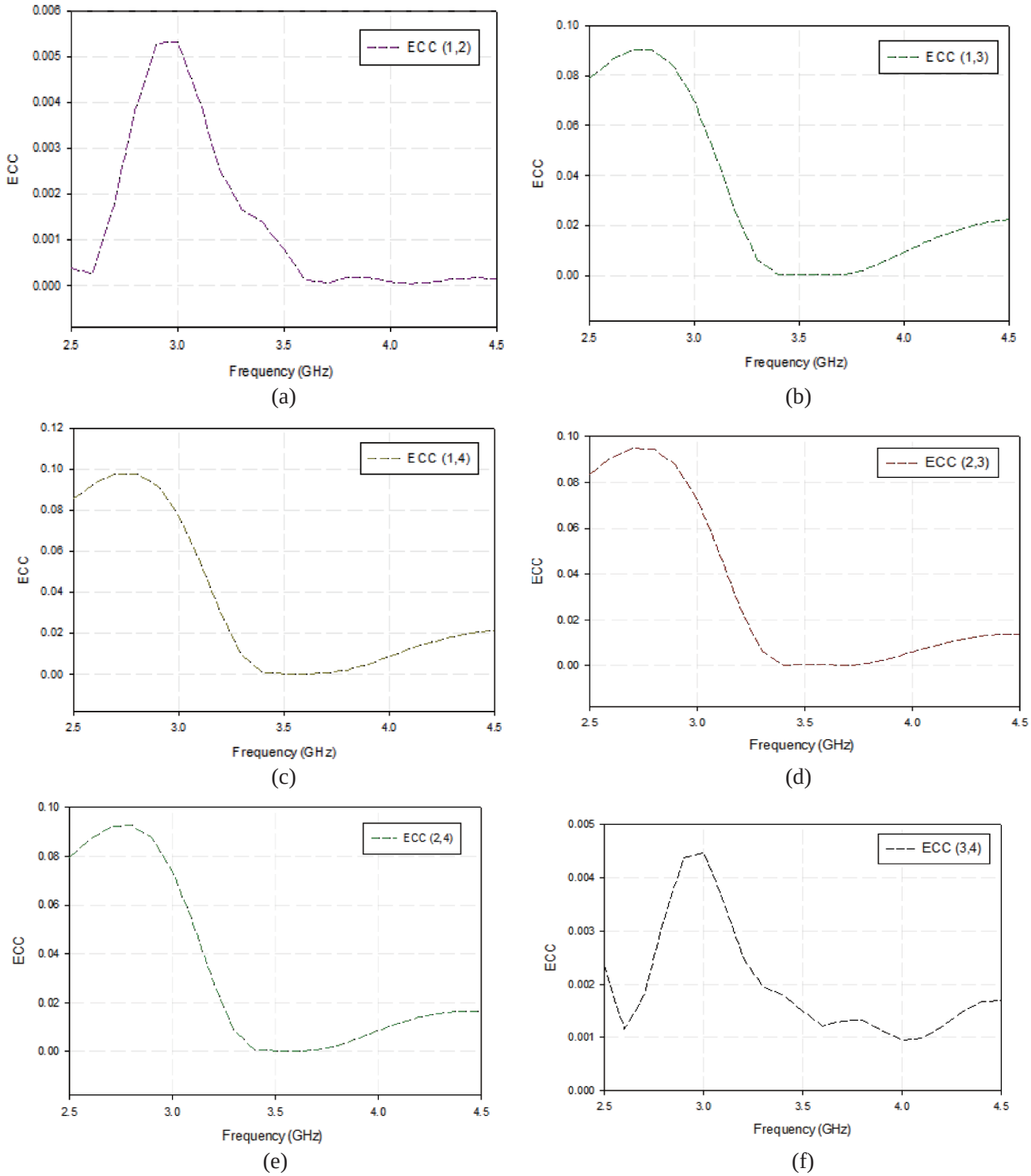

Figure 6. The ECC values of the antenna (a) ECC $(1,2)$, (b) ECC $(1,3)$, (c) ECC $(1,4)$, (d) ECC $(2,3)$ (e) ECC $(2,4)$ and (f) ECC $(3,4)$.

It is given by the formula as given below:

$$\varphi^R = \begin{bmatrix} \rho_{11} & \rho_{12} & \rho_{13} & \rho_{14} \\ \rho_{21} & \rho_{22} & \rho_{23} & \rho_{24} \\ \rho_{31} & \rho_{32} & \rho_{33} & \rho_{34} \\ \rho_{41} & \rho_{42} & \rho_{43} & \rho_{44} \end{bmatrix} \tag{12}$$

where ρ_{ii} and ρ_{ij} are defined as follows

$$\rho_{ii} = 1 - \left| \sum_{n=1}^{N} S_{in} S_{ni} \right| \quad \text{for} \quad i, j = 1, 2, 3 \text{ or } 4 \tag{13}$$

$$\rho_{ij} = 1 - \left| \sum_{n=1}^{N} S_{in} S_{nj} \right| \quad \text{for} \quad i, j = 1, 2, 3 \text{ or } 4 \tag{14}$$

Multiplexing efficiency (ME) is the difference in power required for a MIMO antenna (on test) to achieve a specific throughput compared to the reference standard MIMO antenna. In combination to the diversity parameters described above, the Total Active Reflection Coefficient (TARC) determines the MIMO antenna's efficient operating bandwidth by factoring coupling and random signal configurations. The suggested design's TARC and ME are considerably below -10 dB and less than -1 dB across impedance bandwidth, correspondingly. These figures show that the antenna arrangement presented is appropriate for MIMO applications.

The values of TARC and ME are considered using S-parameters, as presented in the equations below.

$$\text{TARC} = \sqrt{\frac{(S_{11} + S_{12})^2 + (S_{21} + S_{22})^2}{2}} \tag{15}$$

$$\text{ME} = \sqrt{\eta_i \eta_j \left(1 - |\rho_{ij}|^2\right)} \tag{16}$$

where η_i and η_j are the total efficiency of the ith and jth elements, andρ_{ij} is the correlation coefficient between the ith and jth elements.

3. CONCLUSION

For the 5G application, a miniature four-element MIMO antenna is proposed and illustrated. On a minimal FR-4 material, P-shaped radiating elements are generated. The suggested antenna has a small envelope dimension. The referred antenna design has been both calculated and fabricated. At the specified band of 3.4 GHz, both calculations and testing show a return loss of -28 dB. Other results include the envelope correlation coefficient, antenna gain, efficiency, and channel capacity loss, among others. The proposed antenna was also tested, and its efficiency was found to be more effective opposed to the free space antenna design. As a result, the suggested antenna has been demonstrated to be effective to mobile and satellite communications as well as medical applications.

REFERENCES

1. Jensen, M. A. and J. W. Wallace, "A review of antennas and propagation for MIMO wireless communications," *IEEE Trans. Antennas Propag.*, Vol. 52, 2810–2824, 2004.
2. Elfergani, I., A. S. Hussaini, J. Rodriguez, and R. Abd-Alhameed, *Antenna Fundamentals for Legacy Mobile Applications and Beyond*, Springer, New York, NY, USA, 2018.
3. Liao, W. J., C. Y. Hsieh, B. Y. Dai, and B. R. Hsiao, "Inverted-F/slot integrated dual-band four-antenna system for WLAN access points," *IEEE Antenn. Wirel. Pr.*, Vol. 14, 847–850, 2014.
4. Iqbal, A., O. A. Saraereh, A. W. Ahmad, and S. Bashir, "Mutual coupling reduction using F-shaped stubs in UWB-MIMO antenna," *IEEE Access*, Vol. 6, 2755–2759, 2017.
5. Abdullah, M., S. H. Kiani, and A. Iqbal, "Eight element Multiple-Input Multiple-Output (MIMO) antenna for 5G mobile applications," *IEEE Access*, Vol. 7, 134488–134495, 2019.
6. Abdullah, M., S. H. Kiani, L. F. Abdulrazak, A. Iqbal, M. Bashir, S. Khan, and S. Kim, "High-performance Multiple-Input Multiple-Output antenna system for 5G mobile terminals," *Electronics*, Vol. 8, 1090, 2019.

7. Iqbal, A., A. Basir, A. Smida, N. K. Mallat, I. Elfergani, J. Rodriguez, and S. Kim, "Electromagnetic bandgap backed millimeter-wave MIMO antenna for wearable applications," *IEEE Access*, Vol. 7, 111135–111144, 2019.
8. Ahmad, M. S., W. Mohyuddin, H. C. Choi, and K. W. Kim, "4 × 4 MIMO antenna design with folded ground plane for 2.4 GHz WLAN applications," *Microw. Opt. Technol. Lett.*, Vol. 60, 395–399, 2018.
9. Alibakhshikenari, M., M. Khalily, B. S. Virdee, C. H. See, R. A. Abd-Alhameed, and E. Limiti, "Mutual-coupling isolation using embedded metamaterial EM bandgap decoupling slab for densely packed array antennas," *IEEE Access*, Vol. 7, 5182–51840, 2019.
10. Yang, L., T. Li, and S. Yan, "Highly compact MIMO antenna system for LTE/ISM applications," *Int. J. Antennas Propag.*, 714817, 2015.
11. Elfergani, I. and M. Sajedi, "Low profile and closely spaced four element MIMO antenna for wireless body area network," *Electronics*, Vol. 9, No. 2, 258, 2020.
12. Kiem, N. K., H. N. B. Phuong, Q. N. Hieu, and D. N. Chien, "A novel metamaterial MIMO antenna with high isolation for WLAN applications," *Int. J. Antennas Propag.*, Vol. 2015, Article ID 851904, 9 pages, 2015.
13. Singh, H. S., G. K. Pandey, P. K. Bharti, and M. K. Meshram, "A compact dual-band diversity antenna for WLAN applications with high isolation," *Microw. Opt. Technol. Let.*, Vol. 57, 906–912, 2015.
14. Likhitha, T., S. Ashok Kumar, and T. Shanmuganantham, "Design of compact four port MIMO antenna using SRR ring for high isolation," *Proceedings of the International Conference on Antenna Testing and Measurement Society (ATMS 2018)*, 1–4, Pune, India, February 6–7, 2018.